Kirk-Othmer Encyclopedia of Chemical Technology.

ABLATIVE MATERIALS

The word ablation is derived from the suppletive past particle of the Latin *auferre,* which means to remove. It was originally used in the geologic sense to describe the combined, predominantly thermal, processes by which a glacier wastes. The present use of the word maintains the thermal aspect and describes the absorption, dissipation, and blockage of heat associated with high speed entry into the atmosphere. Thus ablative, thermal protection materials are used to protect vehicles from damage during atmospheric reentry. The need for these materials was first realized during the development of operational ballistic missiles in Pennemunde, Germany, when a large percentage of V-2s failed to reach their targets because of missile skin disintegration caused by aerodynamic heating (1). Ablative materials are also used to protect rocket nozzles and ship hulls from propellant gas erosion, as protection from laser beams, and to protect land-based structures from high heat environments.

1. The Ablation Environment

The functional requirements of the ablative heatshield must be well understood before selection of the proper material can occur. Ablative heatshield materials not only protect a vehicle from excessive heating, they also act as an aerodynamic body and sometimes as a structural component (2, 3). Intensity and duration of heating, thermostructural requirements and shape stability (4, 5), potential for particle erosion (6), weight limitations (7–10), and reusability (11) are some of the factors which must be considered in selection of an ablative material.

Some typical ablative environments are shown in Figure 1. Each of the altitude–velocity profiles results in a specific heating rate and radiation equilibrium temperature for a given material. When a vehicle decelerates at high altitudes under low pressure conditions, and the flight angle with respect to the horizon is low, the heating rate is low but the heating time period is long, eg, the Apollo trajectory. In this situation, material insulating ability becomes important. Conversely, a sharp atmospheric entry angle results in severe heating rates but for a shorter duration, eg, the ballistic missile trajectory, which requires less emphasis on the insulating capability of the heatshield material.

Several other factors must also be considered with respect to heating conditions. At the front end of a vehicle, ie, at the nosetip, the heating rate is most severe, generally decreasing toward the aft end of the vehicle in instances of laminar flow. Because of this variation in heating conditions, the nosetip material is usually different from the heatshield or aft end materials. Vehicle design is, of course, influential. Sharp, heavy ballistic vehicles having a high mass-to-drag ratio drop in altitude at higher velocities than blunt, lightweight Apollo-type vehicles, resulting in much higher heating rates for the former. Then also, efficient aerodynamic vehicles, such as long range glide vehicles, utilize sharp leading edges on the nose and wings at the expense of high local heating. Moreover, the rate of heat transfer for a turbulent gas boundary results in higher heating conditions than a laminar gas stream. Thus to reduce or delay the tendency for turbulent flow, smooth, uniform vehicle contours are preferred and, whenever possible, high density materials are avoided to minimize the weight-to-drag ratio.

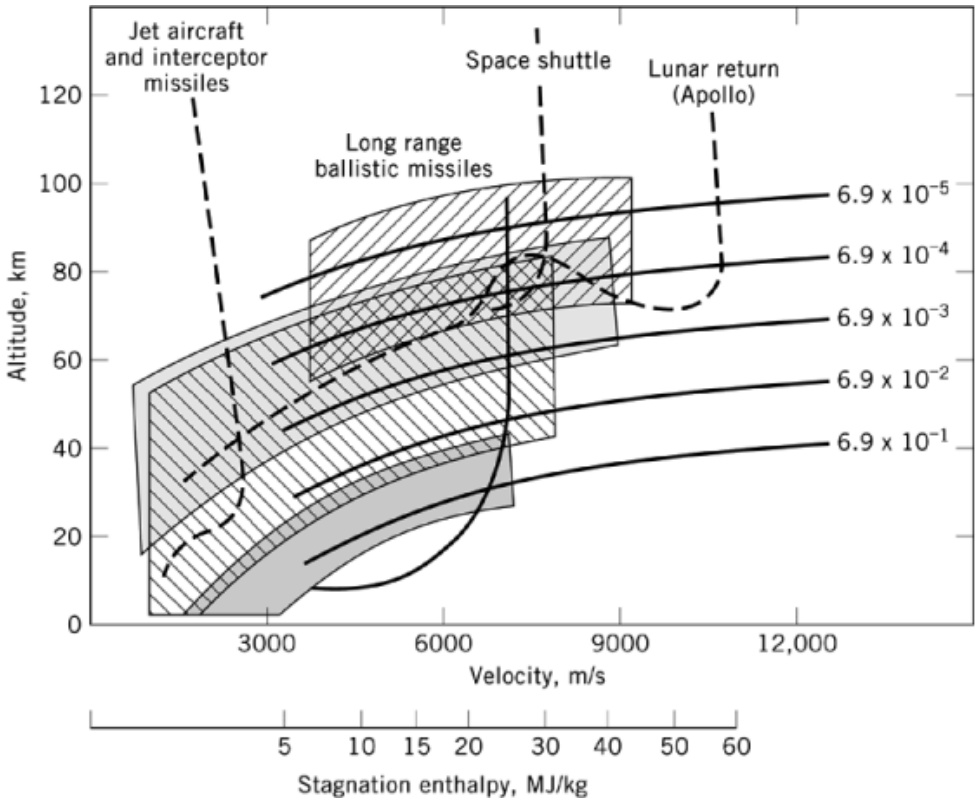

Fig. 1. Simulation facility capabilities and mission requirements: ROVERS arc and 10-MW arc, Textron Defense Systems (TDS); Interaction Heating Facility and Aero Heating Facility, NASA/Ames. Numbers on the curves indicate stagnation pressure P_s in MPa;—, ballistic entry; ___, lifting entry. To convert MPa to psi multiply by 145. To convert MJ to kcal divide by 4.18×10^{-3}.

Heatshield thickness and weight requirements are determined using a thermal prediction model based on measured thermophysical properties. The models typically include transient heat conduction, surface ablation, and charring in a heatshield having multiple sublayers such as bond, insulation, and substructure. These models can then be employed for any specific heating environment to determine material thickness requirements and to identify the lightest heatshield materials.

In a very simplified first-order analysis the ablative heatshield is considered to be of two components: the ablated thickness and the remaining thickness, or the insulation. The ablated weight is determined by the total aerodynamic heat load divided by the heat of ablation, that is, the heat absorbed per unit weight. The insulation weight is determined by the heat conduction parameter, $\rho k/C_p$, the product of density and conductivity, divided by the specific heat, and the ratio of temperature rise at the back surface to that at the front. As shown in Figure 2, the ablated weight increases as the total heat load increases. However, the insulation weight, which initially increases with increased heating, exhibits a maximum and then decreases. Thus at some level ablation begins to dominate, temperature gradients become very steep, and the need for insulation decreases. As a result, the total heatshield weight requirements may not monotonically reflect increases in heat load.

The selection of a material having the right balance of ablation and insulation properties is needed to produce optimum heatshield performance. This material selection is complicated because the higher density

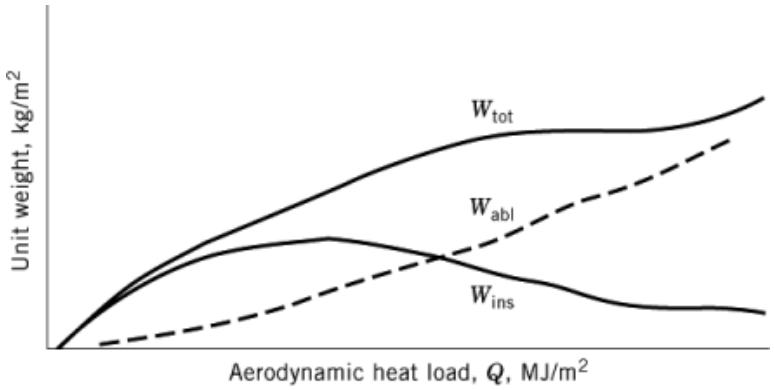

Fig. 2. A simplified material thermal performance analysis for a reentry vehicle thermal protection system where W_{abl}=density×surface recession thickness=total aerodynamic heat/heat of ablation; W_{ins}=density×insulative layer thickness=$f(\rho k/C_p, T_{structure}, T_{surface})$; and W_{tot}=unit weight of heatshield=density×thickness=$W_{abl}+W_{ins}$.

Table 1. Heat of Ablation and Relative Thermal Conductivity for Reentry Vehicle Materials Assuming Laminar Flow

	Cold wall heat of ablation[a], J/g[b]		
Material	H_s = 12,000 J/g[b] V_∞ = 4800 m/s	H_s = 24,000 J/g[b] V_∞ = 6,800 m/s	Relative thermal conductivity
carbon–carbon	32,000	39,500	high
carbon–phenolic	24,000	29,600	⇕
silica–phenolic	13,000	19,000	
Teflon	6,650	10,350	low

[a] H_s is the stagnation enthalpy at the surface of the leading edge; V_∞ is the velocity of the airstream at the leading edge.
[b] To convert J to cal divide by 4.184

materials that usually offer better ablation performance also have higher thermal conductivities and are therefore poor insulators. Properties of known materials are given in Table 1, whereas the desired trends in properties and characteristics of thermal protection (TP) materials are summarized in Table 2 (12). In the high flux region most of the aerodynamic heating is absorbed by ablation. The parameter $\rho k/C_p$ gives some indication of material performance when the rate at which heat is conducted into the shield is very small compared to that at which the heat is radiated away from the surface; ρk alone is somewhat less indicative. Q_{eff} indicates material (and system) performance in all regions because it is essentially a weight parameter including the interaction of all other variables. It must be calculated based on a knowledge of all material properties and mission environment.

The thermostructural requirements of the heatshield are important to material selection and both aerodynamic and attachment load requirements must be met. In the case of a charring ablator, surface char must be of sufficient strength to survive aerodynamic shear. Changes in the ablative material's mechanical and thermal properties occur as a result of the thermal gradient through the depth of the material. Backface surface temperatures, the temperatures on the inside surface of the heatshield, dictate attachment methods and materials. An excessive backface surface temperature caused by inadequate insulation characteristics may weaken an adhesive bond to a substructure or even weaken a load-carrying substructure. In the event that the heatshield also serves as the load-carrying structure, sufficient thickness must be provided for both ablation and insulation so that enough material remains cold (uncharred). A mismatch in axial vs radial thermal

Table 2. Summary of Criteria for Material Selection and Performance Evaluation[a]

Parameter	Definition	Desired trend	Best region of application as a figure of merit
effective heat of ablation[b], q^*	sensible heat + heat of decomposition + mass transfer shielding + shear effects	$\longrightarrow \infty$	High-flux region.
$\frac{\rho k}{C_p}$	$\frac{\text{density} \times \text{conductivity}}{\text{specific heat}}$	$\longrightarrow 0$	Predominant parameter when no ablation occurs.
ρk	density × conductivity	$\longrightarrow 0$	
T_A	ablation temperature	No general trend. Depends on interaction with other parameters and design criteria.	None except as an indicator of whether or not ablation will occur.
T_r	backface temperature	Low or as prescribed.	A design and comparative criterion for testing.
$\epsilon T^4{}_E$	emissivity × (radiation equilibrium temperature)^4	$\epsilon \longrightarrow 1$ depends on interaction with other parameters and design criteria.	Short duration, or when heat leakage into system is minimized.
Q_{eff}[b]	$\frac{\text{total cold wall heat input}}{\text{total required weight of TP system for a given backface temperature}}$	$\longrightarrow \infty$	All regions.
W_t or ρL_t	total required weight of TP system	$\longrightarrow 0$	All regions.

[a] Ref. 12
[b] Also referred to by many other symbols with various heat fluxes as reference.

expansion can result in severe thermal stresses and subsequent failure, as has been noted with the use of thick sections of pyrolitic graphite [7782-42-5] (13, 14). In reentry, erosion from rain or ice particles is also a consideration, particularly at the tip. In addition, in rocket nozzles and on surfaces exposed to propellant gases, erosion resistance from solid particulates must also be considered.

The practice of employing reusable thermal protection systems for reentry is becoming more common. These are essentially ablative materials exposed to environments where very little ablation actually occurs. Examples include the space shuttle tiles and leading edges, exhaust nozzle flaps for advanced engines, and the proposed structural surface skin for the National Aerospace plane.

Another environmental issue important to low earth orbit materials is atomic erosion. At an altitude of 300 km, absorption of solar radiation produces atmospheric temperatures of 1150°C, and at these temperatures gas molecules decompose. Erosion of surface materials by oxygen atoms or nitrogen–oxygen radicals is a serious issue for low altitude orbiting satellites. Experiments conducted on early shuttle flights determined that organic materials that would normally be found on a heatshield erode more rapidly than metallic ones (15). Thus, the effects of atomic erosion must be considered for any vehicle that is subject to long term exposure at low earth altitudes.

A variety of test methods and facilities have been developed to address the process of ablation. These utilize lasers, chemical flames, plasma arcs, electric arc heaters, and other heat sources and sometimes include high velocity wind tunnel facilities that introduce particles to simulate high speed erosion. Examples of ablation facilities used to simulate a variety of reentry conditions are shown in Figure 1. The TDS 10-MW arc facility simulates high speed, high pressure (up to 2.5 MPa) ablation conditions for ballistic reentry. It is mainly used for examining the ablative performance of high velocity nosetip and heatshield materials. The TDS ROVERS (radiation orbital vehicle reentry simulator) arc is a combined convection–radiative heating arc used to simulate

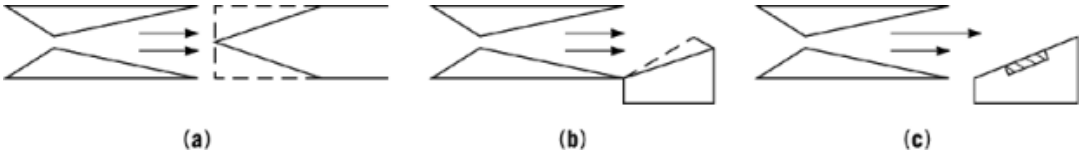

Fig. 3. Simulation parameters (**a**) splash onto cylindrical nosetip; (**b**) attached wedge (—, fixed; ___, varied); and (**c**) detached wedge. See Table 3.

Table 3. Summary of Arc Simulation Capabilities

Parameter	TDS 10-MW arc[a]			TDS ROVERS arc[a]		NASA/Ames Facilities[a,b]	
simulation parameter	splash	detached wedge	attached wedge	splash	detached wedge	Aero Heating	Interaction Heating
cylindrical diameter, cm	to 7.6			to 7.6		20.3	45.7
wedge cutout, cm		5.1×17.8	2.5×7.6		7.6×7.6	66×60	61×61
enthalpy, MJ/kg[c]	0.7–21.2	0.7–21.2	0.7–21.2	0.7–40.2	0.7–40.2	1–31.2	7–44.6
convective heat flux, MW/m^2	1.1–45.4	0.1–7.9	0.6–45.4	0.02–7.9	0.02–7.9	0.006–3.4	0.006–1.5
test time, max, s	20	25	25	continuous	continuous		
gas	air	air	air	air, N_2, others	air, N_2, others	air	air
jet mach no.	1–2	0.5–2.0	1–2.5	2–3.5	2–3.5	2.5–12	5.5–7.5
model surface shear, kg/m^2		4.9–97.6	24.4–488.0		0.2–2.4		
particle erosion	yes	yes	yes				
programmed heating: enthalpy variation	yes	yes	yes	yes	yes		
heat flux variation	yes	yes	yes	yes	yes		
model pressure, MPa[d]	0.1–2.43	0.10–0.51	0.10–0.30	to 0.01	to 0.01	0.0005–0.2	
jet diameter, cm	to 5.1	3.2–5.7	2.5–6.4	to 7.6	to 7.6	7.6–106.7	10^{-5} – 0.0015 to 104.1

[a] See Figure 3 for illustration of simulation parameters.
[b] These facilities can test larger specimens over a wide range of enthalpies and pressures.
[c] To convert MJ to kcal divide by 4.184×10^{-3}.
[d] To convert MPa to psi multiply by 145.

high altitude, low pressure reentry conditions. The Interaction Heating Facility and Aero Heating Facility at NASA/Ames are used to simulate a wide range of pressures and enthalpies and have the capacity for much larger specimen sizes than the Textron facilities. A summary of simulation capabilities is given in Table 3 and Figure 3. A listing of nationwide arc facilities and corresponding test capabilities is also available (16).

2. The Ablation Process

Thermophysically, the ablation process can be described as the elimination of a large amount of thermal energy by sacrifice of surface material. Principles operating during this highly efficient and orderly heat and mass transfer process are (*1*) phase changes such as melting, vaporization, and sublimation, (*2*) conduction and storage of heat in the material substrate, (*3*) absorption of heat by gases as they are forced to the surface, (*4*) heat convection in a liquid layer, (*5*) transpiration of gases and liquids and subsequent heat absorption from

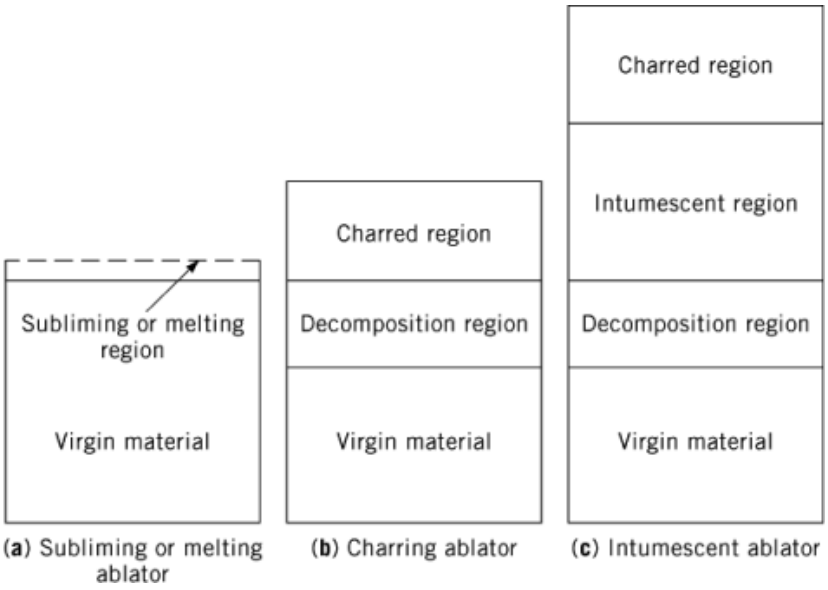

Fig. 4. Physical zones of ablators. Typical time-integrated heat flux, J/m^2, (**a**) 500, (**b**) 5000, (**c**) $_{<50}$; maximum instantaneous heat flux, MW/m^2, (**a**) 0.5, (**b**) $_{>1}$, (**c**) 0.1. To convert J to cal divide by 4.184.

the surface into the boundary layer, (*6*) exothermic and endothermic chemical reactions, and (*7*) radiation on the surface and in bulk (17).

The relationship between heat transfer and the boundary layer species distribution should be emphasized. As vaporization occurs, chemical species are transported to the boundary layer and act to cool by transpiration. These gaseous products may undergo additional thermochemical reactions with the boundary-layer gas, further impacting heat transfer. Thus species concentrations are needed for accurate calculation of transport properties, as well as for calculations of convective heating and radiative transport.

3. Ablative Materials

Ablative materials are classified according to dominant ablation mechanism. There are three groups: subliming or melting ablators, charring ablators, and intumescent ablators. Figure 4 shows the physical zones of each. Because of the basic thermal and physical differences, the classes of ablative materials are used in different types of applications.

3.1. Subliming and Melting Ablators

Subliming ablators act as heat sinks to the incident heat flux until the temperature on the surface reaches the sublimation or melting temperature, also known as the reaction temperature in these cases. At this time the sublimation or melting action removes heat from the insulation material. In the sublimation process the convective transfer of heat from the boundary layer to the material surface is also blocked by the gas evolving from the ablative material, concurrently thickening the boundary layer. This blocking action can reduce the net heating of the ablative material by more than 50%.

Table 4. Bulk Graphite Properties

Material	Specificgravity	% Thermal expansion from 300 to 2500 K	
		Radial, *AB,* direction	Axial, *C,* direction
pyrolytic graphite	2.2	0.5	6
Union Carbide ATJ-S	1.83	0.9	1.2
Unocal Poco AXF-5Q	1.81	1.9	1.9

Some of the early reentry vehicles utilized metallic heat sinks of copper [7440-50-8] or beryllium [7440-41-7] to absorb reentry heat. Other metallic materials that have been evaluated for nosetip applications include tungsten [7440-33-7] and molybdenum [7439-98-7]. The melt layers of these materials are believed to be very thin because of the high rate at which volatile oxide species are formed.

One of the first subliming ablative materials to be identified was polytetrafluoroethylene [9002-84-0], Teflon, which offers light weight, good insulating properties as a result of its decomposition temperature (about 500°C), and a high endothermic value for the depolymerization or ablative heat of reaction. An added advantage is that Teflon ablates to form a volatile monomer without forming a conductive char, thereby maintaining the low dielectric properties of the virgin material. A dielectric material without a conductive char is very useful for transmitting and receiving radiofrequency signals during reentry. For higher heat loads, Teflon and a high temperature dielectric fiber such as quartz can be mixed to reduce the necessary wall thickness and improve overall thermostructural performance. Teflon was proposed as a heatshield for a Venus probe, using a reflective coating on the back end for additional insulation (18). Reinforced Teflon has been suggested for use in high speed ablative missile radome applications (19).

Subliming ablators are used for vehicles subject to long term, low altitude exposure and subsequent atomic erosion. In experiments conducted on early shuttle flights, metallic materials exhibited a significantly greater atomic erosion resistance than organic-based materials with the exception of Teflon, which does not react strongly with atomic oxygen. Very thin coatings of the erosion-resistant materials were found to protect the substrate from atomic erosion. In addition, these coatings sublime cleanly upon reentry (20, 21).

3.1.1. Graphite

Carbon [7440-44-0] has been identified as having the highest heat of ablation. This high ablation efficiency often identifies carbon or carbon composites for use in high heating environments where a minimum of shape change is important, such as in missile nosetips and small radius leading edges. Graphite [7782-42-5] sublimes at temperatures as high as 3900 K (22) (see Carbon, carbon and artificial graphite; Carbon, natural graphite).

When monolithic graphite is used for ablation, the critical factors affecting performance include high uniform density and small uniform pore size. Surface roughening of the graphite, however, caused by ablation down to subsurface porosity, can affect the surface heating as the flow is changed from laminar to turbulent (23). Pyrolitic graphite, which is free of open porosity and very high in density compared to other forms (Table 4), has been shown to be superior in resistance to laser penetration (24). However, pyrolitic graphite exhibits high thermal expansion anisotropy and is therefore subject to thermal fracture. The other commercial forms of graphite are less susceptible to thermal fracture and have also been evaluated for reentry applications. ATJ graphite was found to be an order of magnitude greater in resistance to laser penetration than reinforced charring ablators (25). However, monolithic graphite has been used less in recent years because of the increased variety in forms of reinforced carbon or carbon-carbon composites that are available.

3.1.2. Carbon-Carbon Composites

Carbon–carbon composites are simply described as a carbon fiber reinforcement in one or many directions using a carbon or graphite matrix material (see Composite materials).

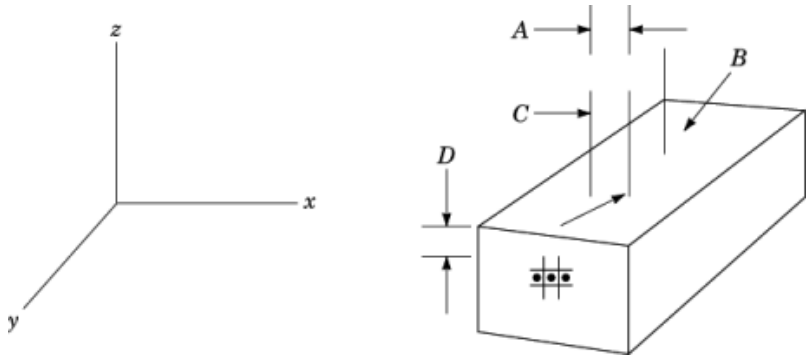

Fig. 5. Unit cell dimensions for carbon-carbon nosetip materials. parameters are

	fine-weave pierced fabric	3D orthogonal weave
A, z: fiber spacing, mm	1.32	0.76
B, z: fiber spacing, mm	1.32	0.76
C, z: fiber size, mm	0.635 diameter	0.38×0.38
D, x, y: cell spacing, mm	0.25	0.86

Techniques available for densifying woven carbon fiber preforms into carbon-carbon composites include (*1*) high pressure impregnation of the preform using molten coal tar or petroleum pitch, followed by pyrolysis and high temperature graphitization for multiple cycles, (*2*) low pressure impregnation using high char yield resin matrices, followed by pyrolysis and graphitization for multiple cycles, and (*3*) carbon vapor deposition-infiltration into the preform using a high strength graphitic structure. Processes are often combined to yield a high density composite (26). These materials exhibit improved thermal stress performance over monolithic graphite.

For nosetip materials 3-directional-reinforced (3D) carbon preforms are formed using small cell sizes for uniform ablation and small pore size. Figure 5 shows typical unit cell dimensions for two of the most common 3D nosetip materials. Carbon-carbon woven preforms have been made with a variety of cell dimensions for different applications (27–33). Fibers common to these composites include rayon, polyacrylonitrile, and pitch precursor carbon fibers. Strength of these fibers ranges from 1 to 5 GPa (145,000–725,000 psi) and modulus ranges from 300 to 800 GPa.

Carbon–carbon composites for rocket nozzles or exit cones are usually made by weaving a 3D preform composed of radial, axial, and circumferential carbon or graphite fibers to near net shape, followed by densification to high densities. Because of the high relative volume cost of the process, looms have been designed for semiautomatic fabrication of parts, taking advantage of selective reinforcement placement for optimum thermal performance.

Other forms of carbon-carbon composites have been or are being developed for space shuttle leading edges, nuclear fuel containers for satellites, aircraft engine adjustable exhaust nozzles, and the main structure for the proposed National Aerospace plane (34). For reusable applications, a silicon carbide [409-21-2] based coating is added to retard oxidation (35, 36), with a boron [7440-42-8] based sublayer to seal any cracks that may form in the coating.

3.1.3. Ceramic Ablators

Several types of subliming or melting ceramic ablators have been used or considered for use in dielectric applications; particularly with quartz or boron nitride [10043-11-5] fiber reinforcements to form a nonconductive char. Fused silica is available in both nonporous (optically transparent) and porous (slip cast) forms. Ford Aerospace manufactures a 3D silica-fiber-reinforced composite densified with colloidal silica (37). The material, designated AS-3DX, demonstrates improved mechanical toughness compared to monolithic ceramics. Other dielectric ceramic composites have been used with performance improvements over monolithic ceramics (see Composite materials, ceramic matrix).

Melting ablators such as nylon and quartz perform essentially as subliming ablators do, except that they melt. In general, melting ablators have heats of reaction similar to subliming ablators but have much higher thermal conductivities. When compared to other types of ablative materials, there are very few advantages to using melting ablators. However, they are often combined with charring ablative materials in a reinforcing fiber form to improve ablation performance by transpirational cooling as the endothermic melt is forced to the surface (38). Some melting ablators have also found application as dielectric ablators, when no electrically conductive residue is formed. Silicon carbide and silicon nitride [12033-89-5] have also been considered as effective ablators for specific thermal protection applications (39).

Subliming ablators are being used in a variety of manufacturing applications. The exposure of some organic polymers to pulsed uv-laser radiation results in spontaneous ablation by the sublimation of a controlled thickness of the material. This photoetching technique is utilized in the patterning of polymer films (40, 41) (see Photochemical technology).

The thermal protection system of the space shuttle is composed mainly of subliming or melting ablators that are used below their fusion or vaporization reaction temperatures (42). In addition to the carbon-carbon systems discussed above, a flexible reusable surface insulation composed of Nomex felt substrate, a Du Pont polyamide fiber material, is used on a large portion of the upper surface. High and low temperature reusable surface insulation composed of silica-based low density tiles are used on the bottom surface of the vehicle, which sees a more severe reentry heating environment than does the upper surface of the vehicle (43).

3.2. Charring Ablators

Charring ablators are used in a greater variety of thermal environments than either subliming or intumescent ablators because of their ability to withstand a much higher heat flux. In the charring ablator, the ablative material acts as a heat sink, absorbing all of the incident heat flux and causing the surface temperature to increase quickly. At reaction temperature, endothermic chemical decomposition occurs: the organic matrix pyrolizes into carbonized material and gaseous products. The passage of heat-absorbing gases through the charred surface provides further insulative performance and thickens the boundary layer, reducing the convective heat transfer. The charring is a continuous process: as the charred surface is eroded by the severe surface environment, more char forms to take its place.

Charring ablators are often used in combination with subliming or melting reinforcement materials. Melting reinforcements such as silica or nylon provide transpirational cooling. Carbon-fiber-reinforced phenolic composites are commonly used as heatshields for high load reentry vehicles (44, 45). This material was also evaluated for survival of the severe heating environment anticipated with the Jovian probe Galileo (46). High strength, high temperature subliming reinforcements such as carbon fibers provide substantial strength, both to withstand high shear environments and to act as a structural heatshield material. A laminated carbon-phenolic composite is typically made by using an 8-harness satin-weave fabric prepreg having fibers at 45° to the wrapping direction (bias orientation) and then laying up on a cylinder or frustum so that the plane of tape makes an angle of 20° to the surface of the shell. This type of configuration improves resistance to delamination, which can occur in a simple cylindrical or scroll wrap. Also, the fibers are at a low angle to the ablating surface,

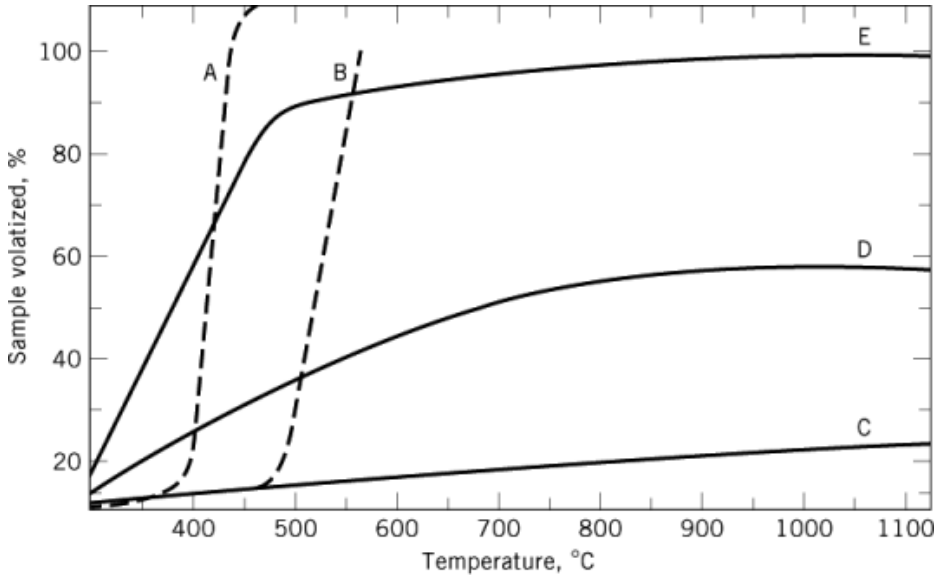

Fig. 6. Decomposition of polymers as a function of temperature during heating. A, polymethylene; B, polytetrafluoroethylene; C, silicone; D, phenolic resin; E, epoxy resin.

thereby minimizing thermal conduction. In some instances the types of reinforcements are varied along the thickness of the material to improve insulation (47) (see Composite materials, polymer matrix).

High density charring ablators such as carbon-phenolic contain high density reinforcements to improve shear resistance. In contrast, lower density charring ablators as a rule are used for low shear environments. The Apollo mission reentry conditions are typical of a relatively low shear environment, so low density ablators consisting of epoxy–novolac resin containing phenolic microballoons and silica fiber reinforcement have been used. In order to improve the shear resistance and safety factor of the material for this mission, the ablator was injected into the cavities of a fiberglass-reinforced phenolic honeycomb that was bonded to the substructure of the craft (48).

Elastomeric shield materials (ESM) have been developed as low density flexible ablators for low shear applications (49). General Electric's RTV 560 is a foamed silicone elastomer loaded with silicon dioxide [7631-86-9] and iron oxide [1317-61-9] particles, which decomposes to a similar foam of SiO_2, SiC, and $FeSiO_3$. Silicone resins are relatively resistant to thermal decomposition and the silicon dioxide forms a viscous liquid when molten (50) (see Silicon compounds, silicones).

One indication of the performance of a charring ablator resin is the ability of the organic material to form a high density char. As shown in Figure 6, silicone is quite resistant to decomposition, even after exposure to high temperatures. Phenolic is also shown to be a relatively high char yield material (50). However, epoxy which has a higher decomposition rate, is commonly used because of ease of handling and processing. In addition, the char structure of epoxy-based ablators can be improved by the addition of a variety of reinforcements (51). For example, a graphite-fiber-reinforced epoxy composite has been found to be a cost-effective substitute for typical low density ablators in a low shear lifting environment (52).

Cork [61789-98-8] is an effective low cost charring ablator. In order to reduce moisture absorption and related poor performance, cork particles are often blended in a silicone or phenolic resin. The result is a uniform ablative material in a sheet form that is easy to apply.

It should be noted that a number of low density ablators contain either glass or phenolic microballoons. Advantages include reduction of the total unit weight of the heatshield and lower thermal conductivity of the base, resulting in improved insulative properties. A very light weight ablative material, composed of glass and phenolic microballoons and cork particles in a silicone resin, has been shown to protect the fuel tank on the space shuttle. A unique gas-injection method was developed to mold the material to the proper configuration (53). Polyurethane foams have also been considered as fuel tank ablative material (54).

Wood has been used as an effective low cost charring ablator. The Chinese successfully used white oak as the heatshield for their RRS FSW vehicle. Wood was recommended as an alternative to more expensive heatshield materials for commercial reusable satellites. However, the safety factors for this type of material should be very high, since there is no easy way to guarantee uniformity. Standard NDT techniques cannot distinguish between cracks and naturally occurring growth rings of various sizes in thick wooden parts.

4. Intumescent Ablators

Additives in an intumescent ablator form a foamlike region on exposure to heat. This process causes the material thickness to increase significantly, resulting in improved insulation performance. Intumescent ablators are sometimes classified as charring ablators because they form a surface char. However, there are several basic differences between intumescent and charring ablators. The basic intumescent decomposition reaction is exothermic, whereas the charring decomposition is endothermic. However, inorganic fillers are usually added to intumescent materials to produce a net endothermic reaction (55). In addition, an intumescent reaction results in decreased thermal conductivity and increased specific heat as the material temperature increases. Conversely, a charring reaction produces a net increase in thermal conductivity and a decrease in specific heat as the material temperature increases. Thus as the net material temperature increases, the thermal diffusivity of an intumescent ablator decreases and that of a charring ablator increases.

The low thermal diffusivity and high depth of penetration make intumescent ablators useful as insulators in transient heat conduction systems. A typical application is as a protective coating for munitions stored on naval ships. In the event of a fire, the insulative properties of the intumescent ablator should provide for more escape time before the munitions detonate from the heat. Intumescent ablators are also used to coat load-carrying beams for bridges, oil rigs, and other structures. The insulative properties of the intumescent ablator should keep the temperatures of the load-carrying beams low, thereby maintaining the high strength of the beam material and delaying the collapse of the structure.

Intumescent ablators are not generally used in severe thermal environments such as reentry, because these materials usually have higher densities than charring ablators and the drastic shape changes they undergo would be detrimental to aerodynamic performance. Intumescent ablators usually possess good mechanical strength, however, and the ablative coating is capable of adding strength to a structure at high temperatures. In some cases a metallic mesh is incorporated to improve resistance of the char to erosive forces.

Several forms of intumescent materials are available from a number of suppliers (56). Some are available as rubberized sheets that can be bonded to simple shaped structures. Others are supplied as a tape, paste, or spray-on coating. A typical example of an intumescent coating material is CHARTEK 59, a high performance, lightweight, epoxy-based material from Textron that can be applied by either spray coating or troweling (57). It adheres well to steel and is used heavily in the hydrocarbon processing industry where protection from high temperature fires is a serious design consideration for support structures. Another example is Interam, a rubber-based intumescent material manufactured by the 3M Co. In one test, Interam was used as a wrap to protect bags of howitzer propellant from heat generated by a nearby explosion. The material successfully prevented ignition of the howitzer propellant, thereby enhancing survival of personnel on military vehicles in the event of a hit in the munitions area (58).

BIBLIOGRAPHY

"Ablation" in *ECT* 2nd ed., Vol. 1, pp. 11–21, by I. J. Gruntfest, General Electric Company; "Ablative Materials" in *ECT* 3rd ed., Vol. 1, pp. 10–26, by E. R. Stover, P. W. Juneau, Jr., and J. P. Brazel, General Electric Company.

Cited Publications

1. D. K. Huzel, *Pennemunde to Canaveral*, Prentice-Hall, Inc., Englewood Cliffs, N.J., 1962.
2. H. J. Allen, *J. Aeronaut. Sci.* **25**, 217 (1958).
3. M. C. Adams, *Jet Propul.* **29**, 625 (1959).
4. A. M. Morrison, *J. Spacecr. Rockets* **12**, 633 (1975).
5. P. J. Schneider and co-workers, *J. Spacecr. Rockets* **10**, 592 (1973).
6. H. L. Moody and co-workers, *J. Spacecr. Rockets* **13**, 746 (1976).
7. D. L. Schmidt in D. V. Rosato and R. T. Schwartz, eds., *Environmental Effects on Polymeric Materials*, Wiley-Interscience, New York, 1968, 487–587.
8. D. L. Schmidt in G. F. D'Alelio and J. A. Parker, eds., *Ablative Plastics*, Marcel Dekker, Inc., New York, 1971, 1–39 (a good reference book) *J. Macromol. Sci. Chem.* **3**, 327 (1969).
9. M. L. Minges in G. F. D'Alelio and J. A. Parker, eds., *Ablative Plastics*, Marcel Dekker, Inc., New York, 1971, 287–313.
10. H. K. Hurwicz, T. Munson, R. E. Mascola, and J. Cordero, *Astronaut. Aerosp. Eng.* **1**(7), 64–73 (Aug. 1963).
11. H. N. Kelley and G. L. Webb, *Assessment of Alternate Thermal Protection Systems for the Space Shuttle Orbiter* (AIAA/ASME 3rd Joint Thermophysics, Fluids, Plasma and Heat Transfer Conference, June 7–11, 1982, St. Louis, Mo., AIAA-82-0899, 1982.
12. Ref. 10, p. 65.
13. C. D. Pears, *Characterization of Several Typical Polygraphites with Some Convergence on Solid Billet ATJ-S* (Proceeding of the Conference on Continuum Aspects on Graphite Design, 1970), CONF-7001105, NTIS, Springfield, Va., 1972, 115–136.
14. J. G. Baetz, *Characterization of Advanced Solid Rocket Nozzle Materials* (SAMSO-TR-75-301), Air Force Rocket Propulsion Laboratories, Edwards AFB, Calif., Dec. 1975.
15. D. E. Hunton, *Sci. Am.* **261**, 92–98 (Nov. 1989).
16. Arnold Engineering Development Center, *Test Facility Data Base, Vol. 3: Aerothermal Test Facilities, Aeroballistic and Impact Ranges, and Space Environmental Chambers*, Arnold Air Force Base, Tenn., Oct. 1988.
17. D. L. Schmidt in ref. 9, p. 5.
18. D. L. Peterson and W. E. Nicolet, *J. Spacecr. Rockets* **11**, 382 (1974).
19. M. R. McHenry and B. Laub, *Ablative Radome Materials Thermal-Ablation and Erosion Modelling* (13th Intersociety Conf. on Environmental Systems, San Francisco, Calif., July 11–13), 1983.
20. S. L. Koontz, K. Albyn, and L. Leger, *Inst. Environ. Sci.* 50–59 (March/April 1990).
21. R. R. Laher and L. R. Megill, *Planet. Space Sci.* **36**, 1497–1508 (1988).
22. H. Hurwicz and J. E. Rogan, "Ablation," in W. M. Rohsenow and J. P. Hartlett, eds., *Handbook of Heat Transfer*, McGraw-Hill Book Co., Inc., New York, 1973, Sect. 16.
23. K. M. Kratsch and co-workers, AFML-TR-70-307, Vol. IV, ASD, Wright-Patterson AFB, Ohio, May, 1973.
24. J. H. Lundell, R. R. Dickey, and J. T. Howe, *Simulation of Planetary Entry Radiative Heating With a CO_2 Gasdynamic Laser* (ASME Conference on Environmental Systems, San Francisco, Calif., July 1975), American Society of Mechanical Engineers, New York, 1975.
25. P. D. Zavitsanos, J. A. Golden, and W. G. Browne, *Study of Laser Effects on Heatshield Materials* (final report), General Electric Co., Philadelphia, Pa., Jan. 1979.
26. J. Delmonte, *Technology of Carbon and Graphite Fiber Composites*, Van Nostrand Reinhold Company, New York, 1981, p. 398.
27. A. R. Taverna and L. E. Mcallister in J. Buckley, ed., *Advanced Materials, Composites and Carbon*, American Ceramic Society, Columbus, Ohio, 1972, 203–211.

28. K. M. Kratsch, J. C. Schutzler, and D. A. Eitman, *Carbon–Carbon 3D Orthogonal Material Behavior* (AIAA Paper No. 72365, AIAA-ASME-SAE 13th Structural Dynamics and Materials Conference, 1972), American Institute of Aeronautics and Astronautics, New York, 1972.
29. E. R. Stover and co-workers, *11th Biennial Conference on Carbon*, CONF-730601, NTIS, Springfield, Va., 1973, pp. 277, 335–336.
30. J. L. Perry and D. F. Adams, *Carbon* **14**, 61 (1976).
31. Product data, Textron Specialty Materials Division, Lowell, Mass., 1990.
32. Product data, Fiber Materials, Inc., Biddeford, Maine, Jan. 1975.
33. J. J. Gebhardt and co-workers, in M. L. Deviney and T. M. O'Grady, eds., *Petroleum Derived Carbons* (ACS Symposium Series No. 21), American Chemical Society, Washington, D.C., 1976, 212–217.
34. J. Brahney, *Aerosp. Eng.* **7**(6) (June 1987).
35. J. M. Williams and R. J. Imprescia, *J. Spacecr. Rockets* **12**, 151 (1975).
36. *Materials,* Office National d'Etudes et de Recherches Aerospatiales, France, 1985, 18–19.
37. T. M. Place, *Proceedings of the 12th Symposium on Electromagnetic Windows*, Georgia Institute of Technology, Atlanta, Ga., 1974, 47–51.
38. H. E. Goldstein in ref. 9, pp. 12, 323.
39. H. Shirai, K. Tabei, and S. Akiba, *JSME Int. J.* **30**(264) 945–949 (1987).
40. R. Srinivasan, *Polym. Degrad. Stab.* **17**(3), 193–203 (1987) *Chem. Abstr.* **107**, 67818u (1987).
41. D. Dijkkamp and A. S. Gozdz, *Phys. Rev. Lett.* **58**(20), 2142–2145 (1987) *Chem. Abstr.* **107**, 40493x (1987).
42. C. D. Lutes, *Nonlinear Modeling and Initial Condition Estimation for Identifying the Aerothermodynamic Environment of the Space Shuttle Orbiter*, Masters thesis, Air Force Institute of Technology, WPAFB, Ohio, Jan. 1984.
43. *A NASA Spinoff Cools the Fire,* NASA Tech Briefs, March, 1988, p. 12.
44. R. W. Farmer, *Extended Heating Ablation of Carbon Phenolic and Silica Phenolic,* AFML-TR-74-75, ASD, WPAFB, Ohio, Sept. 1974.
45. *Ablative Materials Handbook*, U.S. Polymeric, Inc., Santa Ana, Calif., 1964.
46. A. Balkrishnan, W. Nicolet, S. Sandhu, and J. Dodson, *Galileo Probe Thermal Protection: Entry Heating Environments and Spallation Experiment Design*, Acurex Corp./Aerotherm, Mountain View, Calif., Nov. 1979.
47. J. I. Yuck and S. Y. Mo, *Han'guk Somyu Konghakhoechi* **24**(5), 444–452 (1987) (Korean) *Chem. Abstr.* **108**, 132936t (1988).
48. E. P. Bartlett and L. W. Anderson, *J. Spacecr. Rockets* **8**, 463 (1971).
49. T. F. McKeon in ref. 9, 259–286.
50. P. W. Juneau, Jr., *Third Annual Polymer Conference Series, Program VIII, 1972*, University of Detroit, Detroit, Mich., 1972.
51. U.S. Pat. 4,772,495 (Sept. 20, 1988), S. E. Headrick and R. L. Hill (to United Technologies Co.).
52. W. A. Sigur, *SAMPE Q.* **17**(2), 25–33 (1986).
53. K. A. Seeler and L. Erwin, *SAMPE Q.* **17**(3), 40–48 (1986).
54. C. Williams and L. Ronquillo, *Thermal Protection System for the Space Shuttle External Tanks,* 6th SPI Intl., Tech./Mark. Conf., 1983, 90–100.
55. U.S. Pat. 4,088,806 (May 9, 1978), P. W. Sawko and S. R. Riccitiello (to NASA).
56. J. M. Leary, *Characteristics of Various Types of Ablative Materials with Associated Naval Applications*, Thesis, Massachusetts Institute of Technology, Cambridge, Mass., 1983 (a very good reference paper).
57. Product Brochure, Textron Specialty Materials Division, Lowell, Mass., 1990.
58. C. Paone, *Preventing Cook-Off with Intumescent Materials,* Army RD&A Bulletin, Jan.–Feb. 1990.

MICHAEL FAVALORO
Textron Defense Systems

Related Articles

Carbon and artificial graphite, natural graphite; Composite materials, ceramic matrix; Composite materials, polymer matrix